Manipulation and improvement of multiphoton blockade in a cavity-QED system with two cascade three-level atoms

J. Z. Lin,[1,2] K. Hou,[1,3] C. J. Zhu,[1,*] and Y. P. Yang[1,†]

[1]*MOE Key Laboratory of Advanced Micro-Structured Materials, School of Physics Science and Engineering, Tongji University, Shanghai 200092, China*

[2]*Department of Physics, Suzhou Institute of Technology, Jiangsu University of Science and Technology, Zhangjiagang 215600, China*

[3]*Department of Mathematics and Physics, Anhui Jianzhu University, Hefei 230601, China*

We present a study of manipulating and improving the multiphoton blockade phenomenon in a single-mode cavity with two cascade three-level atoms. Using an external control field, we show that the two-photon blockade can be changed to the three-photon blockade by just increasing the control field Rabi frequency when two atoms radiate in-phase. In the case of out-of-phase radiations, we show that the three-photon blockade phenomenon can be significantly improved with an increased mean photon number when the control field is present. We also show that the optical switching from the three-photon blockade [$g^{(2)}(0)>1$ and $g^{(3)}(0)<1$] to the super-Poissonian field [$g^{(2)}(0)>1$ and $g^{(3)}(0)>1$] can be accomplished by increasing the control field Rabi frequency. The results presented in this work provide potential applications in quantum communication and quantum networking.

I. INTRODUCTION

In an atom-cavity QED system driven by a coherent field, a single photon can suppress the transmission of other photons due to the strong coupling between the atom and cavity, which is well known as the two-photon blockade. This phenomenon is a close analogy to the phenomenon of Coulomb blockade [1]. Beyond this, Birnbaum *et al.* demonstrate the photon blockade phenomenon experimentally in a single atom-cavity QED system with strong coupling strength, where the quantum statistic property of the incident photon stream is changed from a Poissonian distribution to sub-Poissonian distribution if the frequency of photons is tuned to one of the states of the lowest doublet dressed states [2].

Due to its potential applications in quantum communication and quantum networking, the study of the two-photon blockade has received extensive attention in the past few decades. Many experimental and theoretical works on photon blockade have been reported in various systems with strong coupling interaction, including the circuit QED systems [3–6], artificial atoms on a chip [7,8], optomechanical systems [9–14], and atom-cavity QED systems [15–23]. Recently, the unconventional photon blockade based on quantum destructive interference also has received a great deal of attention [24] since the two-photon blockade effect can be significantly improved [25–28]. Corresponding experimental works have been reported on the quantum dot cavity QED system [29] and superconducting circuit QED system [30].

Although the two-photon blockade has been studied extensively, the accomplishment of the multiphoton blockade is challenging in experiments. A direct method to realize three-

photon blockade is by increasing the incident field intensity so that two-photon excitations can be measured. However, the strong field intensity will result in the broadening of the dressed states, which compensates the inharmonic energy splitting and prohibits the observation of the three-photon blockade behavior. These characteristics have been observed by Hamsen *et al.* [15]. Another method to realize three-photon blockade is based on the collective decay of two atoms trapped in a single-mode cavity with different coupling strengths [19]. If two atoms have out-of-phase radiations, the three-photon blockade can be achieved since the two-photon excitations are dominant and one-photon excitations are forbidden.

In this paper, we consider that two cascade three-level atoms are strongly coupled in a cavity, where two identical atoms interact with a pump field and a control field simultaneously. The motivation of adding a strong control field is to manipulate the dressed states of the system. We show that the photon blockade behavior can be changed and improved by adjusting the control field intensity. When two atoms radiate in-phase, the two-photon blockade can be changed to the three-photon blockade by increasing the control field Rabi frequency. In the case of out-of-phase radiations, we show that the three-photon blockade can be remarkably improved in the presence of the control field. We also show that it is possible to achieve an optical switching from the three-photon blockade to the super-Poissonian field by increasing the control field Rabi frequency.

II. MODEL AND DRESSED-STATE PICTURE

As depicted in Fig. 1, this two-atom cavity QED system consists of a single-mode cavity and two identical cascade three-level atoms directly driven by a pump field η and a control field Ω_c simultaneously. We assume that the pump (control) field drives the $|g\rangle \leftrightarrow |m\rangle$ ($|m\rangle \leftrightarrow |e\rangle$) transition,

---

*Corresponding author: cjzhu@tongji.edu.cn
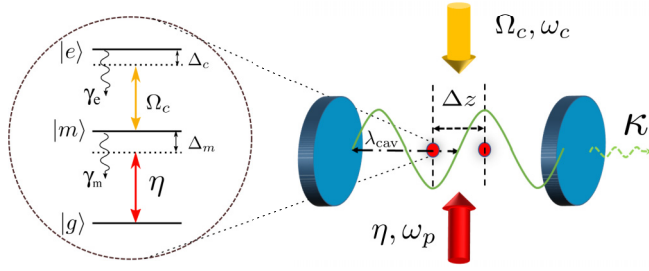
†Corresponding author: yang_yaping@tongji.edu.cn

FIG. 1. Schematic of the two-atom cavity QED system. The wavelength of this single-mode cavity is λ_{cav}, and the corresponding angular frequency is $\omega_{cav} = 2\pi c/\lambda_{cav}$. Each atom has three energy levels labeled as $|g\rangle$, $|m\rangle$, and $|e\rangle$, respectively. A coherent pump field with Rabi frequency η (angular frequency is ω_p) drives the $|g\rangle \leftrightarrow |m\rangle$ transition, and a strong control field with Rabi frequency Ω_c (angular frequency is ω_c) drives the $|m\rangle \leftrightarrow |e\rangle$ transition. The one-photon detunings are defined as $\Delta_m = \omega_m - \omega_g - \omega_p$ and $\Delta_c = \omega_e - \omega_m - \omega_c$. Here, the distance between two atoms is Δz. The spontaneous emission rate of state $|\alpha\rangle$ ($\alpha = m, e$) is γ_α, and the cavity decay rate is κ.

while the cavity mode only couples the $|g\rangle \leftrightarrow |m\rangle$ transition. Clearly, the system is the same as that proposed in Ref. [19] when the control field is turned off (i.e., setting $\Omega_c = 0$).

In general, the dynamical behavior of this cavity-QED system can be described by using the master equation, i.e.,

$$\frac{d\rho}{dt} = -\frac{i}{\hbar}[H, \rho] + \mathcal{L}_\kappa \rho + \mathcal{L}_\gamma \rho, \tag{1}$$

where ρ is the density-matrix operator of the atom-cavity QED system. Under the rotating-wave and electric-dipole approximations, the system Hamiltonian can be written as $H = H_0 + H_I + H_L$ with

$$H_0 = \hbar \sum_{i=1,2} \left(\Delta_e \sigma_{ee}^i + \Delta_m \sigma_{mm}^i + \Delta_{cav} a^\dagger a \right),$$

$$H_I = \hbar \sum_{i=1,2} g_i \left(a\sigma_{mg}^i + a^\dagger \sigma_{gm}^i \right),$$

$$H_L = \hbar \left[\eta \sum_{i=1,2} \left(\sigma_{mg}^i + \sigma_{gm}^i \right) + \Omega_c \sum_{i=1,2} \left(\sigma_{me}^i + \sigma_{em}^i \right) \right],$$

where H_0 is the energy of atoms and the cavity field, H_I represents the interaction between atoms and the cavity field, and H_L is the coherent driving term involving the pump field and control field. The coupling strength between the ith atom and cavity $g_i = g\cos(2\pi z_i/\lambda_{cav})$ depends on the position of the ith atom z_i, where λ_{cav} is the wavelength of the cavity mode (the corresponding angular frequency is $\omega_{cav} = 2\pi c/\lambda_{cav}$). Here, a and $a^\dagger$ are the annihilation and creation operators of the cavity mode, respectively. $\sigma_{jk}^i = |j\rangle^i \langle k|$ ($j, k = \{g, m, e\}$) denotes the atomic operator of the ith atom. The detunings are defined as $\Delta_{cav} = \omega_{cav} - \omega_p$, $\Delta_m = \omega_m - \omega_g - \omega_p$, $\Delta_e = \omega_e - \omega_g - (\omega_p + \omega_c) = \Delta_m + \Delta_c$ with $\Delta_c = \omega_e - \omega_m - \omega_c$ and $\hbar\omega_j$ ($j = \{g, m, e\}$) being the energy of state $|j\rangle$.

The last two terms in Eq. (1) denote the decay of the atoms and cavity, which are given by

$$\mathcal{L}_\kappa \rho = \kappa(2a\rho a^\dagger - a^\dagger a\rho - \rho a^\dagger a), \tag{2}$$

$$\mathcal{L}_\gamma \rho = \sum_{i=1,2} \left[\gamma_e \left(2\sigma_{me}^i \rho \sigma_{em}^i - \sigma_{em}^i \sigma_{me}^i \rho - \rho \sigma_{em}^i \sigma_{me}^i \right) \right.$$
$$\left. + \gamma_m \left(2\sigma_{gm}^i \rho \sigma_{mg}^i - \sigma_{mg}^i \sigma_{gm}^i \rho - \rho \sigma_{mg}^i \sigma_{gm}^i \right) \right], \tag{3}$$

respectively. Here, κ is the cavity decay rate, and γ_α ($\alpha = m, e$) is the spontaneous emission rate of the state $|\alpha\rangle$.

To understand the physical mechanism clearly, we rewrite the Hamiltonian of the system in the dressed-state picture by using $|GG, n\rangle$, $|MG\pm, n-1\rangle$, $|EG\pm, n-1\rangle$, $|MM, n-2\rangle$, $|EM\pm, n-2\rangle$, and $|EE, n-2\rangle$ as the bases in n-photon space (the definitions of these bases are given in the Appendix). Assuming $\Delta_c = 0$ and $\omega_{cav} = \omega_m - \omega_g$ for mathematical simplicity, we have $\Delta_m = \Delta_e = \Delta_{cav} \equiv \Delta_p$. Under the weak-pumping approximation, the effects of the pump field can be treated as a perturbation to the system. Then, the Hamiltonian in one-photon space is expressed as

$$H_{1ph} = \begin{pmatrix} 0 & g_+/\sqrt{2} & g_-/\sqrt{2} & 0 & 0 \\ g_+/\sqrt{2} & 0 & 0 & \Omega_c & 0 \\ g_-/\sqrt{2} & 0 & 0 & 0 & \Omega_c \\ 0 & \Omega_c & 0 & 0 & 0 \\ 0 & 0 & \Omega_c & 0 & 0 \end{pmatrix}, \tag{4}$$

and, in two-photon space, the matrix of the Hamiltonian is given by

$$H_{2ph} =$$
$$\begin{pmatrix} 0 & g_+ & g_- & 0 & 0 & 0 & 0 & 0 & 0 \\ g_+ & 0 & 0 & \Omega_c & 0 & 0 & 0 & \frac{g_+}{\sqrt{2}} & 0 \\ g_- & 0 & 0 & 0 & \Omega_c & 0 & 0 & -\frac{g_-}{\sqrt{2}} & 0 \\ 0 & \Omega_c & 0 & 0 & 0 & \frac{g_+}{2} & -\frac{g_-}{2} & 0 & 0 \\ 0 & 0 & \Omega_c & 0 & 0 & -\frac{g_-}{2} & \frac{g_+}{2} & 0 & 0 \\ 0 & 0 & 0 & \frac{g_+}{2} & -\frac{g_-}{2} & 0 & 0 & \sqrt{2}\Omega_c & \sqrt{2}\Omega_c \\ 0 & 0 & 0 & -\frac{g_-}{2} & \frac{g_+}{2} & 0 & 0 & 0 & 0 \\ 0 & \frac{g_+}{\sqrt{2}} & -\frac{g_-}{\sqrt{2}} & 0 & 0 & \sqrt{2}\Omega_c & 0 & 0 & 0 \\ 0 & 0 & 0 & 0 & 0 & \sqrt{2}\Omega_c & 0 & 0 & 0 \end{pmatrix},$$
$$\tag{5}$$

where $g_\pm = g_1 \pm g_2 = g(1 \pm \cos\phi_z)$ with $\phi_z = 2\pi\Delta z/\lambda_{cav}$.

Diagonalizing Eqs. (4) and (5), we can obtain the corresponding eigenvalues and eigenstates forming the dressed states in one- and two-photon space (see Appendix). Furthermore, we can also obtain the transition strength by calculating the operator $\eta \sum_{i=1,2}(\sigma_{mg}^i + \sigma_{gm}^i)$. These dressed states along with some of the important transitions are shown in Fig. 2, and the physical mechanism of the photon blockade can be understood easily. For example, in the case of $\phi_z = 0$ [i.e., panel (a)], the system can only absorb a single photon to be excited to the one-photon states such as $\Psi_{\pm 2}^{(1)}$. However, the second photon cannot be absorbed due to the inharmonic energy splittings. This phenomenon is widely known as the two-photon blockade. In the case of $\phi_z = \pi$ [i.e., panel (b)], the states in the one-photon space (i.e., $n = 1$) are not allowed
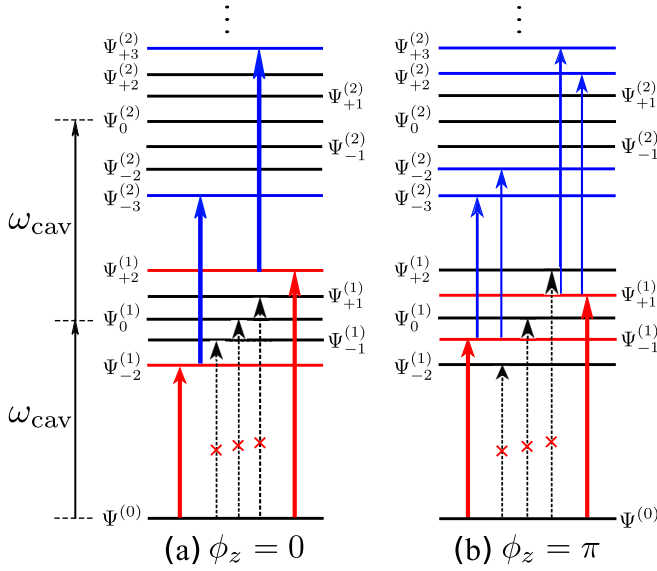
FIG. 2. The dressed-state energy structures for $\phi_z = 0$ [panel (a)] and $\phi_z = \pi$ [panel (b)]. The red arrows represent the one-photon transitions, and the blue ones represent the two-photon transitions. Here, we only show several main pathways of two-photon transitions. The black arrows with red crosses denote that the transitions are forbidden.
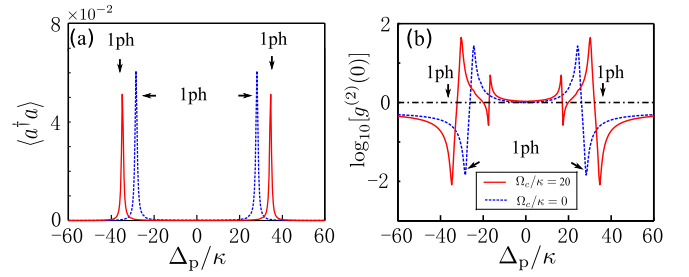

FIG. 3. Panels (a) and (b) display the mean photon number $\langle a^\dagger a \rangle$ and the equal-time second-order field correlation function $\log_{10}[g^{(2)}(0)]$ as a function of the normalized detuning Δ_p/κ, respectively. The Rabi frequency of the control field is chosen as $\Omega_c/\kappa = 0$ (blue dashed curves) and 20 (red solid curves). Other system parameters are given by $\eta/\kappa = 0.2$, $g/\kappa = 20$, $\gamma_m/\kappa = 1$, and $\gamma_e/\kappa = 0.01$. The black dash-dotted line in panel (b) indicates $\log_{10}[g^{(2)}(0)] = 0$.

to be excited because of the destructive interference [19]. Thus, the system can only be excited to the states in the two-photon space (i.e., $n = 2$) via two-photon processes (e.g., $\Psi^{(0)} \to \Psi^{(1)}_{-1} \to \Psi^{(2)}_{-2(-3)}$). Likewise, the third photon cannot be absorbed by the system due to the energy difference. This phenomenon is recognized as the three-photon blockade [19]. In the following, we will show how the control field affects the photon blockade phenomena.

III. THE MANIPULATION OF PHOTON BLOCKADE

Now we focus on the case that the two atoms have the same coupling strengths, i.e., $g_1 = g_2 = g$ leading to $\phi_z = 0$. To show the differences between this three-level atom cavity QED system and the typical two-level atom cavity QED system, we numerically solve Eq. (1) under the condition of a weak pump field.

As shown in Fig. 3, the mean photon number $\langle a^\dagger a \rangle$ [panel (a)] and the equal-time second-order field correlation function $g^{(2)}(0) = \langle a^\dagger a^\dagger aa \rangle / \langle a^\dagger a \rangle^2$ in logarithmic units [panel (b)] are plotted as a function of the normalized detuning Δ_p/κ. Here we choose the control field Rabi frequency as $\Omega_c/\kappa = 0$ (i.e., two-level system, blue dashed curves) and $\Omega_c/\kappa = 20$ (red solid curves), respectively. Other system parameters are chosen as $\eta/\kappa = 0.2$, $g/\kappa = 20$, $\gamma_m/\kappa = 1$, and $\gamma_e/\kappa = 0.01$. For $\Omega_c = 0$, one can observe two peaks in the cavity excitation spectrum at $\Delta_p = \pm\sqrt{2}g$, corresponding to the frequencies of one-photon excitations [i.e., $\Psi^{(0)} \to \Psi^{(1)}_{\pm 2}$ transitions; see the blued dashed curve in panel (a)]. Since the pump field is very weak and one-photon excitations are dominant, the quantum features of the cavity field can be characterized by the second-order correlation function $g^{(2)}(0)$. As shown in Fig. 3(b), the values of $g^{(2)}(0)$ near the one-photon excitation frequencies

are smaller than unity (i.e., $\log_{10}[g^{(2)}(0)] < 0$), which implies that the two-photon blockade behavior and the nonclassical cavity field with sub-Poissonian distribution can be achieved.

For $\Omega_c \neq 0$, the energies of the states $\Psi^{(1)}_{\pm 2}$ shift as the control field intensity increases [see Fig. 2(a) and formulas in the Appendix]. As a result, the width between two peaks in the cavity excitation spectrum $\Gamma_w = 2\sqrt{2g^2 + \Omega_c^2}$ becomes larger than that in the absence of the control field [see the red solid curve in panel (a)]. Compared with the case of $\Omega_c = 0$, the minimum value of $g^{(2)}(0)$ will decrease, corresponding to a slight improvement of the two-photon blockade. The physical mechanism of this improvement attributes to two factors: the energy shifting of the dressed states and the transition strengths. The former causes an increase of the energy difference between states $\Psi^{(1)}_{\pm 2}$ and $\Psi^{(2)}_{\pm 3}$ (the explicit expression is given in the Appendix). Therefore, the second photon becomes much harder to be absorbed by the system. Obviously, adjusting the control field Rabi frequency, one can control the frequency for realizing the two-photon blockade.

Next, we consider the strong-pumping case (e.g., $\eta/\kappa = 1.5$), where the two-photon excitations are as strong as the one-photon excitations. In the absence of the control field, there are four peaks in the cavity excitation spectrum [see Fig. 4(a)], corresponding to the frequencies $\Delta_p = \pm\sqrt{2}g$ (one-photon excitations) and $\Delta_p = \pm\sqrt{6}g/2$ (two-photon excitations), respectively [19]. At frequencies of one-photon excitations, one can obtain $g^{(2)}(0) \approx 0.2$, i.e., the two-photon blockade. Here, the system parameters are chosen as the same as those used in Fig. 3. Near the two-photon excitation frequencies, it is possible to observe the three-photon blockade [i.e., $g^{(2)}(0) > 1$ and $g^{(3)}(0) < 1$] in a narrow regime [see the inserted plot in panel (a)]. It is noted that the observation of the three-photon blockade is challenging in experiments and technique noise becomes a fatal problem because the frequency of the pump field must be controlled precisely. In the presence of the control field (e.g., $\Omega_c/\kappa = 35$), the frequencies for realizing the two- and three-photon blockade phenomena are changed because of the energy shiftings of the dressed states [see Fig. 4(b) and the Appendix].
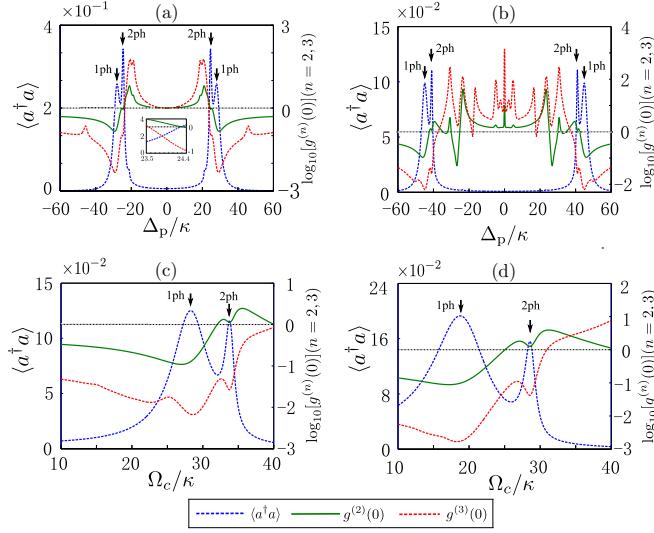
FIG. 4. Plots of the mean photon number (blue dashed curves), equal-time second-order field correlation function $g^{(2)}(0)$ (green solid curves), and third-order field correlation function $g^{(3)}(0)$ (red dashed curves). In panels (a) and (b), the control field Rabi frequency is chosen as $\Omega_c/\kappa = 0$ and $\Omega_c/\kappa = 35$, respectively. The inserted plot in panel (a) shows the frequency regime near the two-photon excitation, and the black dash-dotted lines indicate $g^{(2)}(0) = g^{(3)}(0) = 1$. Here, we choose $\eta/\kappa = 1.5$, $\phi_z = 0$, and the other system parameters are the same as those used in Fig. 3. In panels (c) and (d), we demonstrate an optical switching from the two-photon blockade to the three-photon blockade. The detuning is fixed as $\Delta_p/\kappa = 40$, and the coupling strength $g/\kappa = 20$ in panel (c) and 25 in panel (d).

This feature leads to an optical switching from the two-photon blockade to the three-photon blockade by just increasing the control field Rabi frequency. To show this switching operation, we plot the mean photon number (blue dashed curve) and second-order and third-order field correlation functions (green solid and red dashed curves) as a function of the normalized control field Rabi frequency Ω_c/κ in Fig. 4(c) by fixing the detuning $\Delta_p/\kappa = 40$ and the coupling strength $g/\kappa = 20$. Obviously, the pump field is detuned far away from the one- and two-photon excitation frequencies for weak control field. Increasing the control field intensity, the dressed states are shifted and then the pump field is tuned to be resonant with the state in the one-photon space, leading to the two-photon blockade (see the first peak in the mean photon number). Further increasing the control field intensity, the pump field induces the two-photon excitations. Then, the three-photon blockade can be observed (see the second peak in the mean photon number). In addition, the switch interval, i.e., the interval of the Rabi frequencies of the control field for realizing two- and three-photon blockade, can be enhanced if the coupling strength g increases [see Fig. 4(d)].

IV. SIGNIFICANT IMPROVEMENT OF THE THREE-PHOTON BLOCKADE

Finally, we consider that two atoms have different coupling strengths (i.e., $g_1 = -g_2 = g$ leading to $\phi_z = \pi$). In this case, the two-photon excitations become dominant because $\Psi_0 \rightarrow \Psi_{\pm 1}^{(1)}$ transitions are not allowed [19]. As a result, two
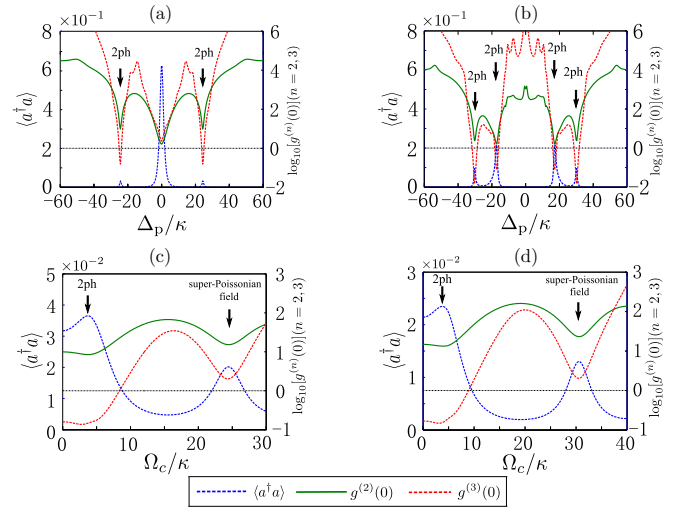
FIG. 5. Panels (a) and (b): Plots of the mean photon number (blue dashed curves) and equal-time second-order (green solid curves) and third-order (red dashed curve) field correlation functions for $\Omega_c/\kappa = 0$ and $\Omega_c/\kappa = 20$, respectively. Here, we choose $\eta/\kappa = 2$, $\phi_z = \pi$, and the other system parameters are the same as those used in Fig. 3. The black dash-dotted line indicates $g^{(2)}(0) = g^{(3)}(0) = 1$. Panels (c) and (d): The demonstration of an optical switching from the three-photon blockade to the super-Poissonian field with fixed detuning $\Delta_p/\kappa = \sqrt{6}g/2$. The coupling strengths are chosen as $g/\kappa = 20$ in panel (c) and $g/\kappa = 25$ in panel (d).

side peaks [see Fig. 5(a)], corresponding to the two-photon excitations $\Psi_0 \rightarrow \Psi_{\pm 1}^{(1)} \rightarrow \Psi_{\pm 3}^{(2)}$ with $\Delta_p = \pm\sqrt{6}g/2$, can be observed in the cavity excitation spectrum when the control field is absent (i.e., $\Omega_c = 0$). Correspondingly, the three-photon blockade [i.e., $g^{(2)}(0) \approx 9.48 > 1$ and $g^{(3)}(0) \approx 0.14 < 1$] occurs at the two-photon excitation frequencies. We also note that the central peak in the cavity excitation spectrum arises from the multiphoton excitation processes [19], which results in $g^{(2)}(0) > 1$ and $g^{(3)}(0) > 1$. In the presence of the control field (e.g., $\Omega_c/\kappa = 20$), there exist four peaks in the cavity excitation spectrum as shown in Fig. 5(b). Examining the dressed states [see Fig. 2(b) and the Appendix], all of them are attributed to the two-photon excitations: $\Psi_0 \rightarrow \Psi_{\pm 1}^{(1)} \rightarrow \Psi_{\pm 2}^{(2)}$ with $\Delta_p = \pm\sqrt{\alpha - \sqrt{\beta}}/(2\sqrt{2})$ and $\Psi_0 \rightarrow \Psi_{\pm 1}^{(1)} \rightarrow \Psi_{\pm 3}^{(2)}$ with $\Delta_p = \pm\sqrt{\alpha + \sqrt{\beta}}/(2\sqrt{2})$. Here, the variables α and β are functions of the control field Rabi frequency Ω_c (see Appendix). Compared with the case of $\Omega_c/\kappa = 0$, it is clear that the mean photon number is enhanced and the three-photon blockade phenomenon can be significantly improved. At the detuning $\Delta_p/\kappa = \pm\sqrt{\alpha + \sqrt{\beta}}/(2\sqrt{2})$, one can obtain $g^{(2)}(0) \approx 2.37$ and $g^{(3)}(0) \approx 1.5 \times 10^{-2}$ with the mean photon number $n \approx 0.1$. We must point out that the value of $g^{(3)}(0)$ is about 10 times smaller than that in the case of $\Omega_c = 0$. The physical mechanism can also be explained by examining the energy difference between the dressed states, where the states in the three-photon space must be considered because of the three-photon processes. In this case, the energy differences for the three-photon absorption $\Delta E_{3ph}^{\pm}$ and $\Delta E_{3ph}'^{\pm}$ gradually increase as the control field intensity increases (see Fig. 6 in the Appendix), which prohibits the absorption of the third
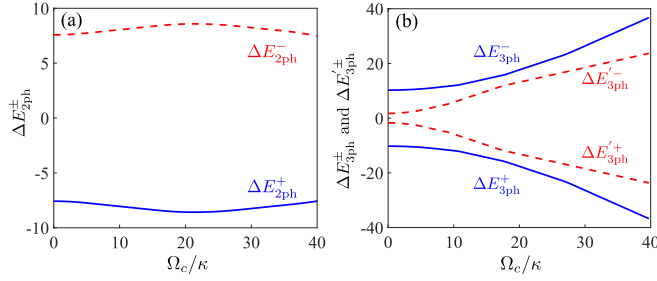
FIG. 6. The energy differences for the two-photon process [panel (a)] and three-photon process [panel (b)]. Here, the coupling strength is $g/\kappa = 20$ and other system parameters are the same as those used in Fig. 3.

photons and leads to a significant improvement of the three-photon blockade.

Based on the above characteristics of the cavity field induced by the control field, we show in Figs. 5(c) and 5(d) that an optical switching from the three-photon blockade to the super-Poissonian field can be accomplished by increasing the control field Rabi frequency. Here, we take the detuning $\Delta_p/\kappa = \sqrt{6}g/2$ and the coupling strengths $g/\kappa = 20$ in panel (c) and $g/\kappa = 25$ in panel (d). Other system parameters are the same as those in Fig. 3. For weak control field, the two-photon transitions are effectively excited so that the three-photon blockade can be observed with $g^{(2)}(0) > 1$ and $g^{(3)}(0) < 1$ [see left peaks in panels (c) and (d)]. Increasing the control field intensity, multiphoton transitions take place so that the super-Poissonian cavity field [$g^{(2)}(0), g^{(3)}(0) > 1$] can be achieved. We also show that the Rabi frequency interval for achieving this optical switching from the three-photon blockade to super-Poissonian cavity field can be enlarged by increasing the coupling strength.

V. CONCLUSION

In summary, we have studied the quantum properties of the cavity field in the atom-cavity QED system with two cascade three-level atoms driven by a pump field and a control field simultaneously. We show that the quantum fluctuations of the cavity field can be controlled by tuning the control field intensity. When two atoms are in-phase radiations, for example, we show that the frequency to realize the two-photon blockade can be actively controlled by adjusting the control field intensity since the dressed states are shifted by the control field. We also show that by increasing the pump field Rabi frequency, not only two-photon blockade but also three-photon blockade can be observed. Fixing the pump field frequency, it is possible to realize an optical switching from the two-photon blockade to the three-photon blockade by just increasing the control field Rabi frequency. In the case of out-of-phase radiations, we show that the three-photon blockade phenomenon can be significantly improved with the enhanced photon number. Furthermore, another optical switching from the three-photon blockade to the super-Poissonian cavity field can be accomplished by increasing the control field Rabi frequency. These results can be realized not only in the atom-cavity QED system but also in the circuit QED system, and may result in potential applications in quantum communication and quantum networking.

APPENDIX: THE EIGENVALUES AND EIGENSTATES OF EQS. (4) AND (5)

The Hamiltonian of the system in the dressed-state picture can be rewritten by using $|GG, n\rangle$, $|MG\pm, n-1\rangle$, $|EG\pm, n-1\rangle$, $|MM, n-2\rangle$, $|EM\pm, n-2\rangle$, and $|EE, n-2\rangle$ as bases in n-photon space, which are defined as

$$|GG, n\rangle = |gg, n\rangle, \quad |MG\pm, n-1\rangle = \frac{1}{\sqrt{2}}(|mg, n-1\rangle \pm |gm, n-1\rangle),$$

$$|EG\pm, n-1\rangle = \frac{1}{\sqrt{2}}(|eg, n-1\rangle \pm |ge, n-1\rangle), \quad |MM, n-2\rangle = |mm, n-2\rangle,$$

$$|EM\pm, n-2\rangle = \frac{1}{\sqrt{2}}(|em, n-2\rangle \pm |me, n-2\rangle), \quad |EE, n-2\rangle = |ee, n-2\rangle.$$

Case 1: $\phi_z = 0$. Diagonalizing Eq. (4), we can obtain the eigenvalues of the dressed states in one-photon space, i.e., $\lambda_0^{(1)} = 0$, $\lambda_{1\pm}^{(1)} = \pm \Omega_c$, and $\lambda_{2\pm}^{(1)} = \pm \sqrt{2g^2 + \Omega_c^2}$, respectively. The corresponding eigenstates are given by

$$\Psi_0^{(1)} = \frac{-\Omega_c}{\sqrt{2}g}|GG, 1\rangle + |EG+, 0\rangle, \quad \Psi_{1\pm}^{(1)} = \pm|MG-, 0\rangle + |EG-, 0\rangle,$$

$$\Psi_{2\pm}^{(1)} = \frac{\sqrt{2}g}{\Omega_c}|GG, 1\rangle \pm \frac{\sqrt{2g^2 + \Omega_c^2}}{\Omega_c}|MG+, 0\rangle + |EG+, 0\rangle.$$

In the two-photon space, the eigenvalues can be obtained by solving Eq. (5), yielding $\lambda_0^{(2)} = \lambda_{0\pm}^{(2)} = 0$, $\lambda_{1\pm}^{(2)} = \pm\sqrt{g^2 + \Omega_c^2}$, $\lambda_{2\pm}^{(2)} = \pm\sqrt{\alpha - \sqrt{\beta}}/\sqrt{2}$, and $\lambda_{3\pm}^{(2)} = \pm\sqrt{\alpha + \sqrt{\beta}}/\sqrt{2}$ with $\alpha = 7g^2 + 5\Omega_c^2$ and $\beta = 25g^4 + 6g^2\Omega_c^2 + 9\Omega_c^4$. Correspondingly, the

eigenstates are given by

$$\Psi_{0+}^{(2)} = \frac{\Omega_c^2}{\sqrt{2}g^2}|GG,2\rangle - \frac{\sqrt{2}\Omega_c}{g}|EG+,1\rangle + |EE,0\rangle, \quad \Psi_{0-}^{(2)} = \frac{\Omega_c^2 - g^2}{\sqrt{2}g^2}|GG,2\rangle - \frac{\sqrt{2}\Omega_c}{g}|EG+,1\rangle + |MM,0\rangle,$$

$$\Psi_0^{(2)} = \frac{-g}{\Omega_c}|MG-,1\rangle + |EM-,0\rangle, \quad \Psi_{1\pm}^{(2)} = \frac{\Omega_c}{g}|MG-,1\rangle \pm \frac{\sqrt{g^2 + \Omega_c^2}}{g}|EG-,1\rangle + |EM-,o\rangle,$$

$$\Psi_{2\pm}^{(2)} = \pm\frac{\gamma + \sqrt{\beta}}{3\sqrt{2}\Omega_c^2}|GG,2\rangle \mp \frac{\sqrt{\alpha - \sqrt{\beta}}(\gamma + \sqrt{\beta})}{12g\Omega_c^2}|MG+,1\rangle - \frac{(\gamma - 6g^2) + \sqrt{\beta}}{6\sqrt{2}g\Omega_c}|EG+,1\rangle \pm \frac{\sqrt{\alpha - \sqrt{\beta}}}{2\Omega_c}|EM+,0\rangle$$

$$+ \frac{-\gamma + 6\Omega_c^2 - \sqrt{\beta}}{6\Omega_c^2}|MM,0\rangle + |EE,0\rangle,$$

$$\Psi_{3\pm}^{(2)} = \frac{-\gamma + \sqrt{\beta}}{3\sqrt{2}\Omega_c^2}|GG,2\rangle \pm \frac{\sqrt{\alpha + \sqrt{\beta}}(-\gamma + \sqrt{\beta})}{12g\Omega_c^2}|MG+,1\rangle + \frac{(-\gamma + 6g^2) + \sqrt{\beta}}{6\sqrt{2}g\Omega_c}|EG+,1\rangle \pm \frac{\sqrt{\alpha + \sqrt{\beta}}}{2\Omega_c}|EM+,0\rangle$$

$$+ \frac{-\gamma + 6\Omega_c^2 + \sqrt{\beta}}{6\Omega_c^2}|MM,0\rangle + |EE,0\rangle,$$

with $\gamma = -5g^2 + 3\Omega_c^2$.

We note that the second pump field photon cannot be absorbed at the detuning $\Delta_p = \lambda_{2\pm}^{(1)}$ due to the energy difference between the states $\Psi_{2\pm}^{(1)}$ and $\Psi_{3\pm}^{(2)}$, which is given by $\Delta E_{2ph}^{\pm} = \lambda_{3\pm}^{(2)} - 2\lambda_{2\pm}^{(1)}$. As shown in Fig. 6(a), the energy differences increase slightly at the beginning, but drop quickly as the control field Rabi frequency increases. Thus, the improvement of the two-photon blockade is very weak as shown in Figs. 4(a) and 4(b).

Case 2: $\phi_z = \pi$. In the one-photon space, the eigenvalues are given by $\lambda_0^{(1)} = 0$, $\lambda_{1\pm}^{(1)} = \pm\Omega_c$, and $\lambda_{2\pm}^{(1)} = \pm\sqrt{2g^2 + \Omega_c^2}$ with the corresponding eigenstates

$$\Psi_0^{(1)} = -\frac{\Omega_c}{\sqrt{2}g}|GG,1\rangle + |EG-,0\rangle, \quad \Psi_{1\pm}^{(1)} = \pm|MG+,0\rangle + |EG+,0\rangle,$$

$$\Psi_{2\pm}^{(1)} = \frac{\sqrt{2}g}{\Omega_c}|GG,1\rangle \pm \frac{\sqrt{2g^2 + \Omega_c^2}}{\Omega_c}|MG-,0\rangle + |EG-,0\rangle.$$

In the two-photon space, we can obtain $\lambda_0^{(2)} = \lambda_{0\pm}^{(2)} = 0$, $\lambda_{1\pm}^{(2)} = \pm\sqrt{g^2 + \Omega_c^2}$, $\lambda_{2\pm}^{(2)} = \pm\frac{\sqrt{\alpha - \sqrt{\beta}}}{\sqrt{2}}$, and $\lambda_{3\pm}^{(2)} = \pm\frac{\sqrt{\alpha + \sqrt{\beta}}}{\sqrt{2}}$. The corresponding eigenstates are given by

$$\Psi_{0+}^{(2)} = -\frac{\Omega_c^2}{\sqrt{2}g}|GG,2\rangle + \frac{\sqrt{2}\Omega_c}{g}|EG-,1\rangle + |EE,0\rangle, \quad \Psi_{0-}^{(2)} = \frac{g^2 - \Omega_c^2}{\sqrt{2}g}|GG,2\rangle + \frac{\sqrt{2}\Omega_c}{g}|EG-,1\rangle + |MM,0\rangle,$$

$$\Psi_0^{(2)} = \frac{g}{\Omega_c}|MG+,1\rangle + |EM-,0\rangle, \quad \Psi_{1\pm}^{(2)} = -\frac{\Omega_c}{g}|MG+,1\rangle \mp \frac{g^2 + \Omega_c^2}{g}|EG+,1\rangle + |EM-,0\rangle,$$

$$\Psi_{2\pm}^{(2)} = \frac{\gamma + \sqrt{\alpha}}{3\sqrt{2}\Omega_c^2}|GG,2\rangle \pm \frac{\sqrt{\alpha - \sqrt{\beta}}(\gamma + \sqrt{\beta})}{12g\Omega_c^2}|MG-,1\rangle + \frac{\gamma - 6g^2 + \sqrt{\beta}}{6\sqrt{2}g\Omega_c}|EG-,1\rangle \pm \frac{\sqrt{\alpha - \sqrt{\beta}}}{2\Omega_c}|EM+,0\rangle$$

$$+ \frac{-\gamma + 6\Omega_c^2 - \sqrt{\beta}}{6\Omega_c^2}|MM,0\rangle + |EE,0\rangle,$$

$$\Psi_{3\pm}^{(2)} = -\frac{-\gamma + \sqrt{\beta}}{3\sqrt{2}\Omega_c^2}|GG,2\rangle \mp \frac{\sqrt{\alpha + \sqrt{\beta}}(-\gamma + \sqrt{\beta})}{12g\Omega_c^2}|MG-,1\rangle - \frac{-\gamma + 6g^2 + \sqrt{\beta}}{6\sqrt{2}g\Omega_c}|EG-,1\rangle \pm \frac{\sqrt{\alpha + \sqrt{\beta}}}{2\Omega_c}|EM+,0\rangle$$

$$+ \frac{-\gamma + 6\Omega_c^2 + \sqrt{\beta}}{6\Omega_c^2}|MM,0\rangle + |EE,0\rangle.$$

To discuss the three-photon blockade, the dressed states in the three-photon space must be considered. In the three-photon space, the Hamiltonian is written as

$$
H_{3\mathrm{ph}} = \begin{pmatrix}
0 & \frac{\sqrt{6}g_+}{2} & \frac{\sqrt{6}g_-}{2} & 0 & 0 & 0 & 0 & 0 & 0 \\
\frac{\sqrt{6}g_+}{2} & 0 & 0 & \Omega_c & 0 & 0 & 0 & g_+ & 0 \\
\frac{\sqrt{6}g_-}{2} & 0 & 0 & 0 & \Omega_c & 0 & 0 & -g_- & 0 \\
0 & \Omega_c & 0 & 0 & 0 & \frac{\sqrt{2}g_+}{2} & -\frac{\sqrt{2}g_-}{2} & 0 & 0 \\
0 & 0 & \Omega_c & 0 & 0 & -\frac{\sqrt{2}g_-}{2} & \frac{\sqrt{2}g_+}{2} & 0 & 0 \\
0 & 0 & 0 & \frac{\sqrt{2}g_+}{2} & -\frac{\sqrt{2}g_-}{2} & 0 & 0 & \sqrt{2}\Omega_c & \sqrt{2}\Omega_c \\
0 & 0 & 0 & -\frac{\sqrt{2}g_-}{2} & \frac{\sqrt{2}g_+}{2} & 0 & 0 & 0 & 0 \\
0 & g_+ & -g_- & 0 & 0 & \sqrt{2}\Omega_c & 0 & 0 & 0 \\
0 & 0 & 0 & 0 & 0 & \sqrt{2}\Omega_c & 0 & 0 & 0
\end{pmatrix}.
$$

The eigenvalues of the above matrix are $\lambda_0^{(3)} = \lambda_{0\pm}^{(3)} = 0$, $\lambda_{1\pm}^{(3)} = \pm\sqrt{2g^2 + \Omega_c^2}$, $\lambda_{2\pm}^{(3)} = \pm\sqrt{X - \sqrt{Y}}/\sqrt{2}$, and $\lambda_{3\pm}^{(3)} = \pm\sqrt{X + \sqrt{Y}}/\sqrt{2}$ with $X = 12g^2 + 5\Omega_c^2$ and $Y = 64g^4 + 24g^2\Omega_c^2 + 9\Omega_c^4$. Correspondingly, the eigenstates are given by

$$
\Psi_{0+}^{(3)} = \frac{-\Omega_c^2}{\sqrt{6}g^2}|GG,3\rangle + \frac{\Omega_c}{g}|EG-,2\rangle + |EE,1\rangle, \quad \Psi_{0-}^{(3)} = \frac{2g^2 - \Omega_c^2}{\sqrt{6}g^2}|GG,3\rangle + \frac{\Omega_c}{g}|EG-,2\rangle + |MM,1\rangle,
$$

$$
\Psi_0^{(3)} = \frac{\sqrt{2}g}{\Omega_c}|MG+,2\rangle + |EM-,1\rangle, \quad \Psi_{1\pm}^{(3)} = \frac{\Omega_c}{\sqrt{2}g}|MG+,2\rangle \pm \frac{\sqrt{2g^2 + \Omega_c^2}}{\sqrt{2}g}|EG+,2\rangle - |EM-,1\rangle,
$$

$$
\Psi_{2\pm}^{(3)} = \pm\frac{Z + \sqrt{Y}}{2\sqrt{6}\Omega_c^2}|GG,3\rangle \pm \frac{\sqrt{X - \sqrt{Y}}(Z + \sqrt{Y})}{12\sqrt{2}g\Omega_c^2}|MG-,2\rangle + \frac{(Z - 12g^2) + \sqrt{Y}}{12g\Omega_c}|EG-,2\rangle \pm \frac{\sqrt{X - \sqrt{Y}}}{2\Omega_c}|EM+,1\rangle
$$

$$
+ \frac{-Z + 6\Omega_c^2 - \sqrt{Y}}{6\Omega_c^2}|MM,1\rangle + |EE,1\rangle,
$$

$$
\Psi_{3\pm}^{(3)} = \frac{Z - \sqrt{Y}}{2\sqrt{6}\Omega_c^2}|GG,3\rangle \pm \frac{\sqrt{X + \sqrt{Y}}(Z - \sqrt{Y})}{12\sqrt{2}g\Omega_c^2}|MG-,2\rangle + \frac{(Z - 12g^2) - \sqrt{Y}}{12g\Omega_c}|EG-,2\rangle \pm \frac{\sqrt{X + \sqrt{Y}}}{2\Omega_c}|EM+,1\rangle
$$

$$
+ \frac{-Z + 6\Omega_c^2 + \sqrt{Y}}{6\Omega_c^2}|MM,1\rangle + |EE,1\rangle
$$

with $Z = -8g^2 + 3\Omega_c^2$.

The absorption of the third photon depends on the energy differences $\Delta E_{3\mathrm{ph}}^{\pm} = \lambda_{3\pm}^{(3)} - 3\lambda_{3\pm}^{(2)}/2$ at the detuning $\Delta_p = \lambda_{3\pm}^{(2)}/2$ and $\Delta E_{3\mathrm{ph}}^{'\pm} = \lambda_{2\pm}^{(3)} - 3\lambda_{2\pm}^{(2)}/2$ at the detuning $\Delta_p = \lambda_{2\pm}^{(2)}/2$. As shown in Fig. 6(b), the energy differences become larger as the control light increases. Thus, it is possible to prevent the system from absorbing the third photon by increasing the control field intensity, resulting in a significant improvement of the three-photon blockade.

[1] A. Imamoğlu, H. Schmidt, G. Woods, and M. Deutsch, Phys. Rev. Lett. **79**, 1467 (1997).

[2] K. M. Birnbaum, A. Boca, R. Miller, A. D. Boozer, T. E. Northup, and H. J. Kimble, Nature (London) **436**, 87 (2005).

[3] A. J. Hoffman, S. J. Srinivasan, S. Schmidt, L. Spietz, J. Aumentado, H. E. Türeci, and A. A. Houck, Phys. Rev. Lett. **107**, 053602 (2011).

[4] Y.-X. Liu, X.-W. Xu, A. Miranowicz, and F. Nori, Phys. Rev. A **89**, 043818 (2014).

[5] X. Wang, A. Miranowicz, H.-R. Li, and F. Nori, Phys. Rev. A **93**, 063861 (2016).

[6] S. Felicetti, D. Z. Rossatto, E. Rico, E. Solano, and P. Forn-Díaz, Phys. Rev. A **97**, 013851 (2018).

[7] A. Faraon, I. Fushman, D. Englund, N. Stoltz, P. Petroff, and J. Vučković, Nat. Phys. **4**, 859 (2008).

[8] A. Reinhard, T. Volz, M. Winger, A. Badolato, K. J. Hennessy, E. L. Hu, and A. Imamoğlu, Nat. Photonics **6**, 93 (2012).

[9] P. Rabl, Phys. Rev. Lett. **107**, 063601 (2011).

[10] M. Ludwig, A. H. Safavi-Naeini, O. Painter, and F. Marquardt, Phys. Rev. Lett. **109**, 063601 (2012).

[11] J.-Q. Liao and F. Nori, Phys. Rev. A **88**, 023853 (2013).

[12] D. Hu, S.-Y. Huang, J.-Q. Liao, L. Tian, and H.-S. Goan, Phys. Rev. A **91**, 013812 (2015).

[13] H. Xie, C.-G. Liao, X. Shang, M.-Y. Ye, and X.-M. Lin, Phys. Rev. A **96**, 013861 (2017).

[14] G.-L. Zhu, X.-Y. Lü, L.-L. Wan, T.-S. Yin, Q. Bin, and Y. Wu, Phys. Rev. A **97**, 033830 (2018).

[15] C. Hamsen, K. N. Tolazzi, T. Wilk, and G. Rempe, Phys. Rev. Lett. **118**, 133604 (2017).

[16] I. Schuster, A. Kubanek, A. Fuhrmanek, T. Puppe, P. W. Pinkse, K. Murr, and G. Rempe, Nat. Phys. **4**, 382 (2008).

[17] A. Kubanek, A. Ourjoumtsev, I. Schuster, M. Koch, P. W. H. Pinkse, K. Murr, and G. Rempe, Phys. Rev. Lett. **101**, 203602 (2008).

[18] J. A. Souza, E. Figueroa, H. Chibani, C. J. Villas-Boas, and G. Rempe, Phys. Rev. Lett. **111**, 113602 (2013).

[19] C. J. Zhu, Y. P. Yang, and G. S. Agarwal, Phys. Rev. A **95**, 063842 (2017).

[20] M. J. Werner and A. Imamoğlu, Phys. Rev. A **61**, 011801(R) (1999).

[21] S. Rebić, A. S. Parkins, and S. M. Tan, Phys. Rev. A **65**, 063804 (2002).

[22] J.-Q. Liao and C. K. Law, Phys. Rev. A **82**, 053836 (2010).

[23] A. Miranowicz, M. Paprzycka, Y.-x. Liu, J. Bajer, and F. Nori, Phys. Rev. A **87**, 023809 (2013).

[24] T. C. H. Liew and V. Savona, Phys. Rev. Lett. **104**, 183601 (2010).

[25] A. Majumdar, M. Bajcsy, A. Rundquist, and J. Vučković, Phys. Rev. Lett. **108**, 183601 (2012).

[26] M. Bamba, A. Imamoğlu, I. Carusotto, and C. Ciuti, Phys. Rev. A **83**, 021802(R) (2011).

[27] D. Gerace and V. Savona, Phys. Rev. A **89**, 031803(R) (2014).

[28] H. Flayac and V. Savona, Phys. Rev. A **96**, 053810 (2017).

[29] C. Vaneph, A. Morvan, G. Aiello, M. Féchant, M. Aprili, J. Gabelli, and J. Estève, Phys. Rev. Lett. **121**, 043602 (2018).

[30] H. J. Snijders, J. A. Frey, J. Norman, H. Flayac, V. Savona, A. C. Gossard, J. E. Bowers, M. P. van Exter, D. Bouwmeester, and W. Löffler, Phys. Rev. Lett. **121**, 043601 (2018).